

# Real-Time Location-Aware Demand-Shaping for Power-Constrained AC Railway Corridors

Márton László Ambrus, Xiao Liu, Stuart Hillmansen, and Zhongbei Tian

**Abstract**—Power-constrained 25 kV AC railway sections, particularly under degraded feeding, are protected today by blunt, section-wide power limits that penalise every train irrespective of whether it contributes to the binding condition. This paper presents a real-time, location-aware controller that restores the electrical feasibility of a feeding section with minimal impact on the timetable: it curtails only the trains that bind, where and when they bind, evaluating feasibility and per-train available power online with a solver-free estimate as an in-loop surrogate for the full power flow. Because the estimate is accurate on average but slightly optimistic at the binding instants, the controller screens with a small voltage margin, and a full multi-conductor power-flow solver confirms the restored feasibility. The resulting selective-curtailment policy is delivered through a cloud-to-edge connected driver advisory system. On a representative GB 25 kV corridor under outage feeding, solver-selected to be infeasible uncontrolled yet restorable, the controller is compared against the uncontrolled case, the incumbent static limit, and an offline genetic-algorithm optimum, with every feasibility figure solver-validated. The static limit restores feasibility at a large journey-time cost by throttling the whole section; the location-aware controller restores the same feasibility at one thirtieth of that cost by advising a single train, and matches the offline optimum’s solution in about a second and a half against the optimiser’s minute. Aggregate peak demand is unmoved, because the active constraint is local far-field voltage rather than gross demand. All claims are relative to the baselines on a representative corridor; a specific-route deployment study is future work.

**Index Terms**—AC railway, traction power, demand-side management, driver advisory systems, real-time control, power-flow estimation, decarbonisation.

## I. INTRODUCTION

**E**LECTRIFICATION of the railway is central to transport decarbonisation, yet on parts of the GB network the electrical supply is the binding constraint on what traffic can be run on electric power rather than diesel [1], [2]. Where a feeding section is weak, most acutely when a substation is out and the section is fed from one end, the catenary voltage falls as trains draw power, and operators protect the supply by limiting traction power. In current practice this limit is *blunt*: a fixed reduction applied across the whole constrained section, to every train, for the duration of its transit, regardless of whether that train is responsible for the depressed voltage at any instant.

That bluntness is wasteful, and the reason is structural. The minimum section voltage is governed not by aggregate

power but by the sum, over the trains sharing a segment, of the product of each train’s power and its electrical distance from the supply [3]. The binding condition is therefore caused by particular trains, at particular locations, during particular overlaps of their high-power windows. A static, section-wide limit ignores this entirely, throttling a lightly loaded train near the supply exactly as much as a heavily loaded train far out, and so spending far more journey time than the electrical relief it buys. Operational measurements show the signature of this inefficiency directly: a blunt limit sharply reduces the short-window (one-minute) RMS demand while barely changing the long-window (thirty-minute) RMS, and hence the energy drawn [4]. The energy is merely spread in time, which is what a demand-side controller seeks, but achieved by the most expensive available means.

This paper asks whether the same supply protection can be obtained at a fraction of the journey-time cost by limiting only the trains and instants that bind. The obstacle to doing so online has been computational: identifying the binding trains requires evaluating the multi-train power flow, and a full solver is too slow to run inside a control loop over a forecast horizon. A companion paper [3] removed that obstacle with a solver-free estimate of the power available to each train on a feeding section, accurate enough and fast enough to be queried repeatedly online. The present paper builds the controller that acts on that estimate, and evaluates it.

The contributions are: (i) a control formulation that casts supply protection as restoring compliant supply voltage ( $V_{\min} \geq U_{\min}$ ) at the smallest necessary journey-time penalty, with feasibility and available power evaluated online by the estimate of [3] (Section IV); (ii) a transparent, executable selective-curtailment policy that screens with a small voltage margin to remain robust to the estimate’s optimism at the binding instants, and its delivery through a cloud-to-edge C-DAS architecture (Section IV); and (iii) a case study on a representative GB 25 kV corridor under outage feeding, selected with the full power-flow solver in the loop and with every feasibility figure solver-validated, comparing the controller against the uncontrolled case, the incumbent static limit, and an offline GA optimum, with every parameter traceable to a standard or cited source (Sections V–VII, with the scoring and validation procedure in Section VI). Section VIII discusses validity and deployment, and Section IX concludes.

## II. BACKGROUND AND RELATED WORK

**Energy-efficient train control.** A large literature optimises a single train’s speed profile for energy, from the optimal-control foundations through to practical advisory systems [5],

This work was supported by RSSB (project T1366). (Corresponding author: M. L. Ambrus)

The authors are with the Birmingham Centre for Railway Research and Education, University of Birmingham, Birmingham, U.K. (e-mail: m.l.ambrus@bham.ac.uk)

[6], [7], [8], [9]. Multi-train extensions coordinate several trains, typically for energy or regenerative exchange, and jointly optimise speed profile and timetable [10], [11], [12], [13]; broader assessments catalogue the measures available to reduce network traction energy [14]. These methods largely treat the electrical supply as adequate; the problem here is the opposite: the supply is the constraint, and the objective is to protect it with minimal impact on the timetable.

**Power-flow-coupled optimisation.** Where the supply is modelled, optimisation is generally offline, coupling a timetable optimiser to a railway power-flow solver [15], [12]. Offline DP and GA methods can approach the true optimum with full future knowledge [16], [17], [18], but cannot run within live-traffic timescales, and their raw schedules are volatile and hard for a driver to follow. Accelerating AC power flow for online use is an active topic in the wider power-systems literature, building on the classical optimal-power-flow formulation [19], [20], [21], [22], [23]; the estimate of [3] is the railway-specific counterpart exploited here.

**Driver advisory systems.** Connected DAS deliver online advice to drivers and are increasingly deployed [24]. The gap this paper addresses is that no deployed DAS shapes *multi-train* demand using a *location-aware* estimate of available power, in real time, under supply constraint. A systematic review of algorithmic energy management in constrained traction networks situates this gap [25].

### III. SYSTEM MODEL AND AVAILABLE-POWER ESTIMATE

The corridor is modelled as a sequence of feeding sections delimited by neutral sections; within a section the catenary, rails and (where present) autotransformers form a multi-conductor chain circuit solved by a fixed-point AC power flow [26], [27], [28]. Each train is a complex power injection at its instantaneous position, subject to the voltage-dependent automatic current limitation (ACL) of EN 50388-1: the permissible current derates once the pantograph voltage falls below  $V_1 \approx 19$  kV and is fully suppressed below  $V_0 \approx 12.5$  kV, while  $U_{\min} = 17.5$  kV is the EN 50163 compliance limit between them [29], [30]. Train motion follows the standard distance-domain equations, with tractive effort limited by the lesser of adhesion and power-over-speed. This solver is both the model to which the companion estimate [3] is calibrated and the ground truth against which every committed plan is judged (Section V).

The physics the controller exploits is captured by one relation. For a train at distance  $d$  from the supply point drawing active power  $P$  at pantograph voltage  $V$ , on a feeder of series resistance  $r$  per unit length, the resistive voltage drop is approximately

$$V_s - V \approx r d \frac{P}{V}, \quad (1)$$

so the depression scales with the *product* of power and distance, and when several trains share the feeder their drops superpose over the shared path [3]. Which train binds therefore depends on where each train is, not merely on how much it draws, the structural fact a section-wide limit ignores.

#### A. Solver-free available-power estimate

The control loop of Section IV does not call the solver online. Instead it uses the solver-free estimate of [3], whose operative form is reproduced here so that the present paper is self-contained. For  $N$  trains at distances  $d_i$  drawing complex powers  $S_k = P_k(1 + j\kappa)$ , with  $\kappa$  fixed by the displacement factor, the train voltages satisfy the shared-path relation

$$V_i = V_s - \sum_k M_{ik} \left( \frac{S_k}{V_k} \right)^*, \quad (2)$$

$$M_{ik} = \gamma(d_i, d_k) Z(\min(d_i, d_k)),$$

in which  $Z(d) = Z_0 + \beta(d)zd$  is the calibrated series impedance from the supply point to distance  $d$ , and  $\gamma(d_i, d_k) = \gamma_\infty + (1 - \gamma_\infty)e^{-|d_i - d_k|/L} \leq 1$  (with  $\gamma \equiv 1$  on the diagonal) is a separation-dependent mutual coupling-reduction factor. The generalisation of (1) that invalidates any additive headroom rule is thus retained: train  $k$ 's current depresses train  $i$ 's voltage through the feeder length the two share back to the supply point. Both terms are calibrated offline, per feeding configuration: a single-train solver sweep fixes the self-impedance profile  $\beta(d)$ , and a small set of two-train sweeps fits  $(\gamma_\infty, L)$ ; for the single-end-fed corridor used here,  $\gamma_\infty \approx 0.02$  and  $L \approx 3.4$  km. Online, (2) is solved by a damped fixed point in a few  $\mathcal{O}(N^2)$  iterations, returning the section minimum voltage  $V_{\min} = \min_i |V_i|$ ; a bisection on train  $i$ 's power, re-solving (2) at each trial, returns the power  $H_i$  available to train  $i$  before  $V_{\min}$  reaches  $U_{\min}$ . Both are obtained without a power-flow solve, at a cost that scales with the number of trains rather than with the network, low enough to evaluate repeatedly inside a controller.

Against matched multi-train power-flow snapshots the estimate reproduces the per-train available power to a mean absolute deviation of about 9% (maximum 16.6%), as a tight two-sided approximation that runs slightly optimistic for distant, lightly loaded trains [3], precisely the configuration that decides feasibility on a single-end-fed section, which is why the controller of Section IV screens with a voltage margin. We take  $V_{\min}$  and  $H_i$  from this estimate as the controller's in-loop evaluator of feasibility and headroom, and reserve the full solver for offline ground-truth validation of the chosen control.

### IV. DEMAND-SHAPING CONTROL

#### A. Formulation

Let  $P_i(t)$  be the traction power of train  $i$  (negative when regenerating) and  $\mathcal{P}(t) = \sum_i P_i(t)$  the aggregate demand presented to the section. With the  $\tau$ -window RMS

$$\overline{\mathcal{P}}_\tau(t) = \sqrt{\frac{1}{\tau} \int_{t-\tau}^t \mathcal{P}(s)^2 ds}, \quad (3)$$

the short window  $\tau_1$  (one minute) tracks the instantaneous stress that depresses voltage, and the long window  $\tau_{30}$  (thirty minutes) tracks the energy the substation rating must accommodate.

On a power-constrained section under outage feeding, the binding operational limit is not the aggregate demand but the catenary voltage: normal traffic drives  $V_{\min}$  below  $U_{\min}$  in the far field, so the section is *infeasible*. The controller's objective

is therefore to restore feasibility with minimal impact on the timetable, to choose the per-train profiles  $\{P_i\}$ , within the operational freedom the timetable allows, that

$$\min_{\{P_i(\cdot)\}} \sum_i \Delta T_i \quad (4)$$

subject to, for every train  $i$  and time  $t$ ,

$$V_{\min}(t) \geq U_{\min}, \quad P_i(t) \leq H_i(t), \quad \Delta T_i \leq \Delta T_{\max}, \quad (5)$$

together with the train-dynamics relations linking  $P_i$  to motion and arrival time. Here  $\Delta T_i$  is the journey-time penalty of train  $i$  relative to its unconstrained run and  $\Delta T_{\max}$  the tolerance (tens of seconds). The feasibility and headroom constraints in (5) are evaluated by the estimate of [3], which is what makes the problem solvable online; and because  $H_i$  is location-aware, the controller caps only the binding trains rather than the whole section.

The peak short-window RMS  $\overline{P}_{\tau_1}$  of (3) is retained as a *secondary* demand-shaping indicator. It responds when the binding condition coincides with the aggregate-demand peak, but on a section whose voltage binds far from the feed it can be largely unaffected even as feasibility is fully restored, because the aggregate peak is a whole-line sum while the binding is local. We report it, and return to this distinction in Section VIII.

### B. Selective curtailment policy

The general solution of (4)–(5) is a constrained optimisation over the joint cap choice. We adopt a transparent, deterministic policy that exposes the mechanism and is cheap enough to run online, in two passes (Fig. 1). The policy is *non-anticipative*: trains are processed in the order they enter the constrained band, and a train’s cap is decided at its entry, when the capped and uncapped profiles still coincide and the advice is actionable.

In the *restriction pass*, each train in turn is checked by evaluating the estimate over its traversal of the band; while the predicted section minimum voltage is below  $U_{\min}$ , the train’s cap is tightened one level and the traversal re-checked, until it is feasible or the deepest cap is reached. This restores feasibility but over-caps, because an early train forecasts against a still-uncapped future. The *relaxation pass* then loosens each train’s cap to the least restrictive level that keeps its traversal feasible given the others, and repeats until no cap changes, a fixed point at which every train carries only the curtailment the others do not already provide. Because curtailment is concentrated on the binding trains and instants, its journey-time cost falls where it does electrical work, in contrast to the section-wide penalty of a static limit. Both passes use only the estimate, so the whole decision costs milliseconds; the relaxation is a planning-time iteration, so the issued advice remains a single stable figure per train.

*Screening margin.* The estimate tracks the full power flow closely on average (Section III), but runs optimistic at the most heavily loaded far-field instants, exactly those that decide feasibility (Section VII). A controller that screened at  $U_{\min}$  directly would therefore under-cap, leaving a residual breach

the solver would still see. We close this by screening against  $U_{\min} + \Delta$  with a fixed margin  $\Delta$  (here 1.5 kV): the restriction and relaxation passes both target  $U_{\min} + \Delta$  in the estimate, so that the true minimum voltage clears  $U_{\min}$  once the solver is consulted. The margin is the honest, quantified price of using a fast estimate near the limit rather than a solver in the loop; its journey-time cost is small (Section VII).

### C. Executability and C-DAS delivery

Advice that changed every second would be electrically optimal and operationally useless. The controller therefore commits a power figure over a section and time window, rate-limited and held with hysteresis, expressed in terms the driver already uses. It is delivered through the cloud-to-edge C-DAS of Fig. 2: a central (cloud) function forecasts the binding state with the estimate and emits a section power parameter; the on-train (edge) C-DAS recomputes a normal speed/coast advisory under that parameter, which the driver follows, shaping the train’s traction-power draw. Train telemetry (position, speed, power) returns to the central function to close the forecast loop. The control boundary is one-way and read-only: the central function sets a parameter, never a direct command. The device degrades gracefully on loss of connectivity by holding its last valid parameter, and no new advisory class is introduced. This is the deployment vehicle, not the contribution.

## V. CASE STUDY SETUP

### A. Representative corridor

The corridor is a representative GB 25 kV AC section under degraded (N–1) feeding: 100 km, direct-fed from one end, with paralleling posts and a representative line impedance, voltages and current-limitation characteristic per EN 50163 and EN 50388-1. No single real route is reproduced; every parameter is traceable to a standard or to the cited AC-supply literature [31], [32], [33], [26], so the corridor is a defensible composite. Table I lists the parameters and their provenance. The route carries a bidirectional peak-hour timetable of one high-speed and five regional services at four-minute headway. The traffic level was chosen *with the full power-flow solver in the loop*, by sweeping headway, mix and count and retaining a case the solver confirms is genuinely infeasible uncontrolled, its far-field voltage dipping below  $U_{\min}$  without collapsing, yet restorable by curtailing the binding train. This matters: the online estimate is optimistic at the binding instants, so a scenario selected on the estimate alone can read as restorable while the solver shows it collapsed; selecting on the solver avoids that trap and makes every feasibility figure below solver-backed. The single high-speed service is the binder. Its high-power far-field pass, thickened by regional overlap, drives the dip, and the binding band sits at 52–76 km.

### B. Baselines and metrics

The controller is compared against four references: the *uncontrolled* case (nominal profiles, no management); the *static section limit*, reproducing the incumbent blunt reduction (every train capped to 0.85 of rated power for its transit of the

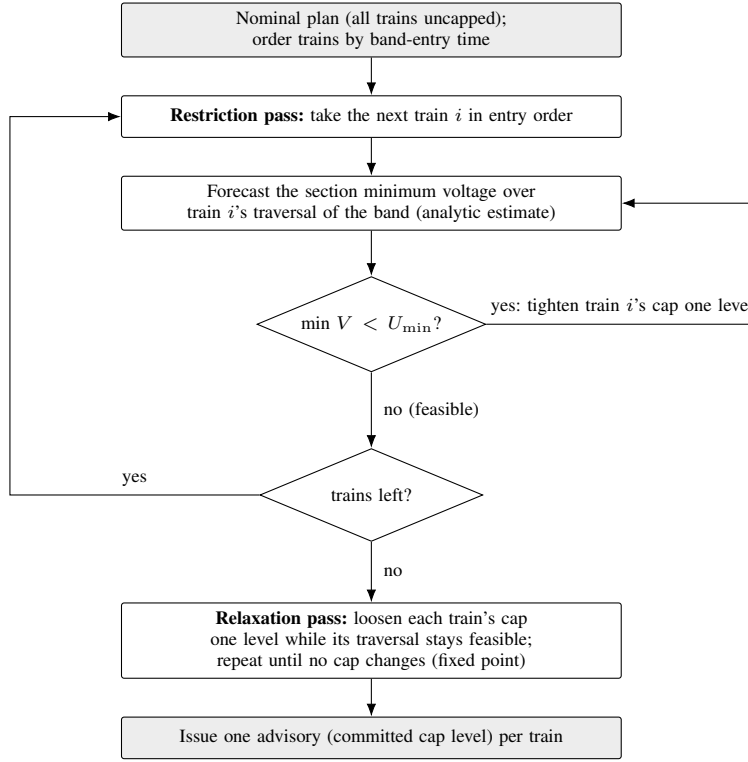


Fig. 1. Online controller logic. A non-anticipative restriction pass restores feasibility train-by-train at band entry; a relaxation pass then removes the over-capping by loosening each cap to the least restriction the rest of the traffic allows. Both passes query only the analytic estimate, so the plan is computed in milliseconds.

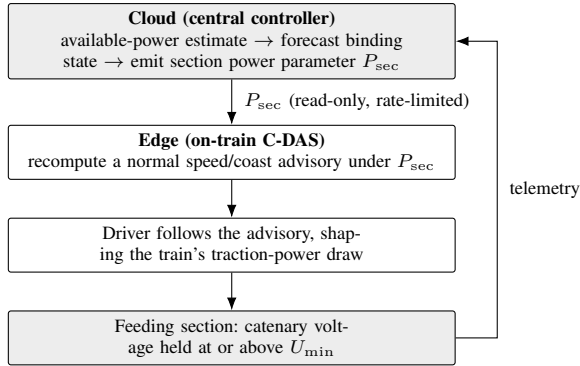


Fig. 2. Cloud-to-edge C-DAS delivery. The central function forecasts the binding state from the available-power estimate and pushes a single section power parameter  $P_{sec}$  to each train; the on-train C-DAS turns it into a normal driving advisory, and train telemetry (position, speed, power) returns to close the forecast loop. The boundary is one-way and read-only, and the edge holds its last valid parameter if the link drops.

TABLE I  
REPRESENTATIVE CORRIDOR PARAMETERS AND PROVENANCE.

Parameter	Value	Source
Voltages ( $V_{oc}/V_n/U_{min}$ )	27.5 / 25 / 17.5 kV	EN 50163 [29]
ACL onset / cut-off	19 / 12.5 kV	EN 50388-1 [30]
Power factor	0.96	EN 50388-1 [30]
Feeding	single-end, DF (outage)	repr. [26]
Section length	100 km	repr. (matched to route)
Line speed	160 km/h	typical GB main line
Station spacing	~33 km	typical GB intercity
Gradients	$\leq 10\%$	within GB ruling grades
Rolling stock	1 high-speed, 5 regional	published characteristics
Headway	/ 240 s	/ solver-selected (Sec. V)
directions	bidirectional	

section); the *offline GA optimum*, a strong reference computed with full future knowledge [16], [17]; and the proposed *online controller*. Metrics follow the objective: constraint-violation duration, i.e. the number of seconds with  $V_{min} < U_{min}$  (primary: feasibility restoration is the task); total journey-time penalty  $\sum_i \Delta T_i$  (the cost of restoring it); decision runtime (the real-time test); and the number of trains advised and cap depth (advice volatility, the executability measure). Peak one-minute RMS of (3) is reported as a secondary demand-shaping indicator.

The comparison tests two pre-stated hypotheses.  $H_{1a}$ : the online controller restores feasibility at least as well as the incumbent static limit, at lower total journey-time cost.  $H_{1b}$ : the online controller matches the offline GA optimum's feasibility and cost, in real time and with few advisories. Both are decided on solver voltages (Table IV).

### C. Validation strategy

All evaluation is in-simulation; the sim-to-real gap is a declared limitation, not a hidden assumption. Within that

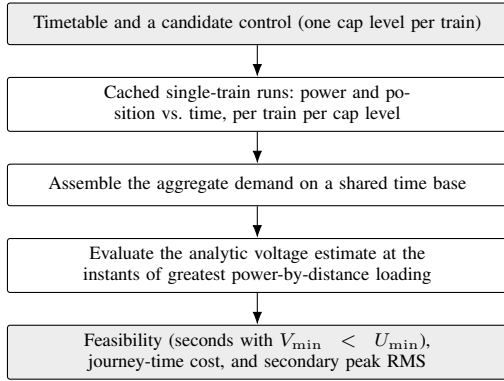


Fig. 3. Scoring a candidate control. Single-train runs are simulated once and cached, so evaluating a control is a table lookup and one estimate pass, not a re-simulation, which is what makes the online search tractable.

scope, the network model is anchored to an independent baseline established in prior RSSB work on network-wide traction-energy management [34] rather than to its own self-consistency [4], and the controller is benchmarked against the *real* incumbent measure rather than a strawman. Crucially, feasibility is not asserted from the online estimate: every committed plan (uncontrolled, static, GA and controller) is re-scored second by second by the full multi-conductor AC power-flow solver, and it is those solver voltages, not the estimate’s, that appear in the results (Section VII). The estimate is used only online, to *form* the control; the solver is the judge. To keep the static and GA baselines like-for-like with the controller, all three screen against the same  $U_{\min} + \Delta$  margin. All claims are relative; absolute MW figures for any specific real route are out of scope.

## VI. COMPUTATIONAL PROCEDURE

Every candidate control is a choice of one cap level per train from the discrete set of Section V. It is scored as in Fig. 3: the aggregate demand is assembled from the constituent single-train runs on a shared time base, and the analytic estimate of Section III is evaluated at the instants of greatest power-by-distance loading. Feasibility is the number of seconds at which the estimated section minimum voltage falls below  $U_{\min}$ , and cost is the summed journey-time penalty relative to the unconstrained runs. The single-train runs are produced once per train per cap level by a distance-domain traction simulator that applies the section power cap, and cached, so that scoring a candidate is a lookup and an estimate evaluation rather than a re-simulation, which is what keeps the controller and the baselines tractable. The binding band is located automatically as the stretch of track occupied by the trains that dominate the lowest-voltage instants. The static limit, the offline GA and the online controller all draw from this same cached set and the same estimate, screening at the same  $U_{\min} + \Delta$  margin, so their comparison is like-for-like. Runtime (Table II) is the wall-clock cost of forming the control decision, the estimate evaluations and ranking, measured against the GA’s total search time on the same scenario.

Two uses of the full multi-conductor solver sit around this fast inner loop. First, the scenario itself is *selected* with the

TABLE II  
HEADLINE METRICS ACROSS BASELINES, *solver-validated*. PRIMARY AXES ARE FEASIBILITY (SECONDS WITH  $V_{\min} < U_{\min}$ ) AND JOURNEY-TIME COST; MINIMUM VOLTAGE AND RUNTIME SUPPORT THEM; PEAK ONE-MINUTE RMS IS A SECONDARY INDICATOR. THE STATIC, GA AND CONTROLLER PLANS ALL SCREEN AT THE SAME  $U_{\min} + \Delta$  MARGIN ( $\Delta = 1.5$  kV).

Baseline	Infeas. (s)	$\sum \Delta T_i$ (s)	Min $V$ (kV)	Runtime
Uncontrolled	57	–	16.35	–
Static limit	0	210	19.26	–
Offline GA	0	7	19.01	64.9 s
<b>Online (this work)</b>	<b>0</b>	<b>7</b>	<b>19.01</b>	<b>1.45 s</b>

Peak one-minute RMS is 8.98 MW for every policy (Section VIII); the online controller advises 1 train (the high-speed service), one cap level.

TABLE III  
ESTIMATE AGAINST THE FULL SOLVER: SECTION MINIMUM VOLTAGE PER COMMITTED PLAN, EVALUATED ON THE SAME SECOND-BY-SECOND SNAPSHOTS. THE ESTIMATE IS OPTIMISTIC BY ONLY 0.2 kV AT THE BINDING (UNCONTROLLED) CONFIG BUT BY UP TO 1.5 kV ONCE THE TRAINS ARE LIGHTLY CAPPED, WHICH IS WHY THE CONTROLLER SCREENS WITH A 1.5 kV MARGIN. THE THREE CONTROLLED PLANS EACH REGISTER ZERO INFEASIBLE SECONDS BECAUSE EACH RESTORES COMPLIANCE ACROSS THE WHOLE HORIZON; ONLY THE UNCONTROLLED CASE BREACHES, AND ESTIMATE AND SOLVER AGREE ON THAT VERDICT FOR EVERY PLAN.

Policy	Est. min $V$ (kV)	Solver min $V$ (kV)	Solver infeas. (s)
Uncontrolled	16.57	16.35	57
Static limit	20.71	19.26	0
Offline GA	20.55	19.01	0
Online controller	20.55	19.01	0

solver: candidate traffic levels are swept and each is scored by the solver uncontrolled, retaining one that is genuinely infeasible yet convergent rather than one the estimate merely reports as infeasible. Second, every committed plan is *re-scored* by the solver second by second over the whole horizon, and it is those voltages that populate Tables II and III. The estimate forms the control; the solver judges it. The controller, estimator, baselines, solver harness and representative corridor are available from the authors on request.

## VII. RESULTS

*Every figure in Table II is the full solver’s verdict on the committed plan, over the whole horizon at one-second resolution; the estimate’s value is shown alongside in Table III to quantify its accuracy. On this corridor there is no voltage collapse under any policy (the scenario was selected to be infeasible but supplyable), so the infeasible-second count is a clean measure of the task.*

**Reading.** Under outage feeding the uncontrolled section is infeasible for 57 s: its far-field voltage falls to 16.35 kV, below the 17.5 kV limit, though it does not collapse (Table II, Fig. 4). That is the motivation: normal peak traffic cannot be supplied within compliance. The incumbent static limit restores feasibility, but bluntly: capping every train to 0.85 lifts the minimum to 19.26 kV at a cost of 210 s of aggregate journey time, because it throttles five trains that never bind

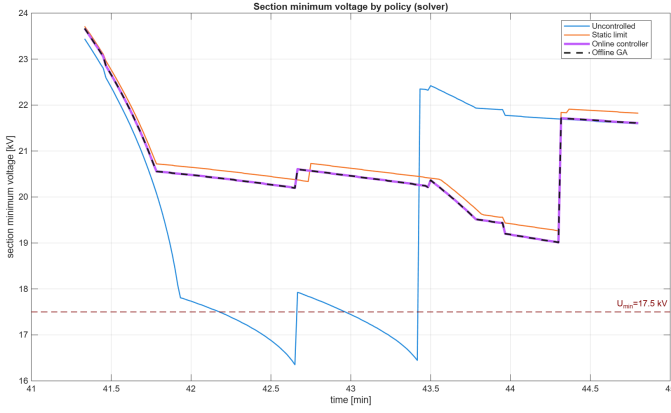


Fig. 4. Section minimum voltage under each policy, from the full power flow, over the binding window (the corridor is comfortably above  $U_{\min}$  outside it). The uncontrolled section dips to 16.35 kV, below the 17.5 kV compliance line; the static limit, the GA and the online controller all hold above it, the GA (dashed) and controller tracing the same trajectory because they commit the same cap. There is no collapse: feasibility is restored, not a collapse merely softened. This is the result the paper turns on.

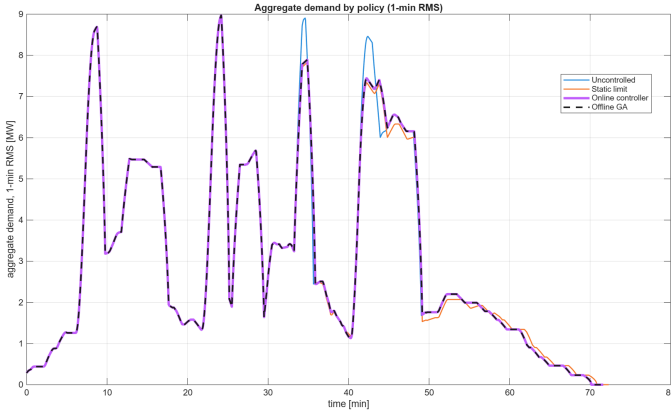


Fig. 5. Aggregate demand (one-minute RMS) under each policy; the offline GA is drawn dashed over the online controller, which commits the identical plan. The peak (8.98 MW) is the same for every policy: curtailing the far-field binding train does not move the whole-line aggregate peak, which occurs elsewhere on the corridor, even as feasibility is restored (Fig. 4). Within the binding window the static limit reduces demand most, as it caps all six trains there, whereas the controller and GA reduce it only where the single binding train is curtailed. This is the secondary “binding is local” observation of Section VIII made visible.

alongside the one that does. The offline GA restores the same feasibility (19.01 kV) for 7 s, and it does so by capping the single high-speed service (the binder) one level. The online controller returns the *identical* plan, 19.01 kV for 7 s advising that one train, computed in 1.45 s against the GA’s 64.9 s. The controller thus dominates the incumbent on cost at equal feasibility ( $H_{1a}$ , 30 $\times$ ) and reaches the offline optimum in real time ( $H_{1b}$ ); that the GA independently commits the same cap is the strongest available check that the controller is not cutting a corner. Peak one-minute RMS is 8.98 MW for every policy: curtailing the far-field binder does not move the whole-line aggregate peak, which sits elsewhere on the corridor, the point developed next.

TABLE IV  
HYPOTHESIS OUTCOMES, SOLVER-VALIDATED.  $H_{1a}$ : ONLINE CONTROLLER VS INCUMBENT STATIC LIMIT.  $H_{1b}$ : ONLINE CONTROLLER VS OFFLINE GA OPTIMUM.

Hypothesis	Test	Outcome
$H_{1a}$	Restores feasibility at least as well as the static limit, at lower journey cost	Yes: both feasible (0 vs 0 s), 7 vs 210 s cost, a 30 $\times$ reduction, one train advised vs the whole section
$H_{1b}$	Matches the offline optimum’s feasibility and cost, in real time, with few advisories	Yes: identical plan (0 vs 0 s, 7 vs 7 s cost), 1.45 s vs 64.9 s runtime, 1 train advised

## VIII. DISCUSSION

**The active constraint is local, not aggregate.** The most instructive observation is that peak one-minute RMS is 8.98 MW under every policy while feasibility varies from 57 to 0 infeasible seconds. Aggregate demand is a whole-line sum, but the voltage binds locally, in the far field where impedance from the single-end feed is greatest; curtailing the one train that binds restores feasibility without materially changing the aggregate. For a power-constrained outage section, then, the quantity to manage is far-field voltage feasibility, not gross demand. A blunt demand cap, which acts on the aggregate, is aimed at the wrong target, which is why it costs so much more journey time than the location-aware cap for the same relief (210 s vs 7 s). **The estimate is accurate on average but optimistic at the limit.** Table III shows the online estimate tracking the solver to within 0.2 kV at the binding config and about 1.5 kV once the trains are lightly capped, consistent with the estimator’s reported accuracy [3], but always on the optimistic side, and most so at the heavily loaded instants that decide feasibility. A controller that trusted the estimate at  $U_{\min}$  would therefore under-cap and leave a residual breach. Screening at  $U_{\min} + \Delta$  closes this: with  $\Delta = 1.5$  kV the controller’s true minimum voltage is 19.01 kV, comfortably compliant, at a journey-time cost of only 7 s. The margin is the honest, quantified price of a solver-free online screen near the limit, and it is small. **Where it helps.** Location-aware curtailment helps most when the binding is concentrated in identifiable trains, here a single high-speed service; it approaches the static limit only when loading is uniform, so no small set of trains dominates the power-by-distance sum. **Threats to validity.** The study is in-simulation; per-train power and voltage are inferred from position and speed rather than measured. The result is a single, solver-selected scenario; its purpose is to establish that location-aware curtailment restores *genuine* (solver-confirmed) feasibility more cheaply than a blunt cap, and a robustness study across traffic levels and binding locations is future work. The controller is sequential and non-anticipative: it commits each train’s cap at band entry using only information available then and does not revise earlier commitments, so in denser cases a train already in the band when a later one binds cannot be re-advised, a residual the offline optimum

could in principle avoid; here the two coincide exactly, so no residual arises, but it bounds the guarantee in general. **Operational implication.** Restoring feasibility by targeted curtailment rather than blanket limiting releases the journey time a blunt cap wastes, here a factor of thirty, which is what would let more traffic, including bi-mode services on electric power, run on a constrained section without a supply upgrade, complementing hardware measures such as wayside energy storage [35].

## IX. CONCLUSION

In this paper we proposed a near real-time, location-aware controller that restores the electrical feasibility of a power-constrained AC section by curtailing only the trains that bind, using the solver-free available-power estimate of [3] as an in-loop surrogate for the full power flow, screened with a small voltage margin so that the solver confirms compliance, and delivered through a cloud-to-edge C-DAS. On a representative GB 25kV corridor under outage feeding, selected with the solver in the loop and evaluated entirely on solver voltages, the incumbent static limit restored feasibility only by throttling the whole section for 210 s of journey time, whereas the controller restored the same feasibility for 7 s by advising a single train, a thirtyfold reduction, and reached the offline optimum's exact solution in 1.45 s against its minute. A secondary finding is that on such a section the active constraint is local far-field voltage rather than aggregate demand, so a blunt demand cap acts on the wrong quantity; a third is that the online estimate, while accurate on average, is optimistic at the binding instants, which a fixed screening margin corrects at small cost. The result is established on a single, solver-selected scenario against real incumbent and theoretical baselines; a robustness study across traffic levels and binding locations, a specific-route (e.g. East Coast Main Line) deployment study, and a learned controller for the full receding-horizon problem, for example via multi-agent reinforcement learning [36], are future work.

## REFERENCES

- [1] Department for Transport, "Decarbonising transport: A better, greener Britain," Department for Transport, London, UK, Tech. Rep., 2021.
- [2] Network Rail, "Traction decarbonisation network strategy: Interim programme business case," Network Rail, London, UK, Tech. Rep., 2020.
- [3] M. L. Ambrus, X. Liu, S. Hillmansen, and Z. Tian, "Estimating available traction power in multi-train ac railway networks from a distance-dependent power envelope," 2026. [Online]. Available: <https://arxiv.org/abs/2606.28948>
- [4] RSSB, "Review of AC electric rolling stock power limitations," Rail Safety and Standards Board, London, UK, Tech. Rep. T1331, 2025, research project, 2024–2025.
- [5] G. M. Scheepmaker, R. M. Goverde, and L. G. Kroon, "Review of energy-efficient train control and timetabling," *European Journal of Operational Research*, vol. 257, no. 2, pp. 355–376, 2017.
- [6] A. Albrecht, P. Howlett, P. Pudney, X. Vu, and P. Zhou, "The key principles of optimal train control—part 1: Formulation of the model, strategies of optimal type, evolutionary lines, location of optimal switching points," *Transportation Research Part B: Methodological*, vol. 94, pp. 482–508, 2016.
- [7] S. Lu, S. Hillmansen, T. K. Ho, and C. Roberts, "Single-train trajectory optimization," *IEEE Transactions on Intelligent Transportation Systems*, vol. 14, no. 2, pp. 743–750, 2013.
- [8] Z. Tian, N. Zhao, S. Hillmansen, C. Roberts, T. Dowens, and C. Kerr, "Smartdrive: Traction energy optimization and applications in rail systems," *IEEE Transactions on Intelligent Transportation Systems*, vol. 20, no. 7, pp. 2764–2773, 2019.
- [9] X. Liu, Y. Peng, Z. Tian, S. Lu, L. Jiang, and M. Chen, "Comparative performance analysis of speed trajectory optimization algorithms for metro and high-speed railways," *IEEE Transactions on Transportation Electrification*, 2025.
- [10] N. Zhao, C. Roberts, S. Hillmansen, and G. Nicholson, "A multiple train trajectory optimization to minimize energy consumption and delay," *IEEE Transactions on Intelligent Transportation Systems*, vol. 16, no. 5, pp. 2363–2372, 2015.
- [11] S. Su, T. Tang, and C. Roberts, "A cooperative train control model for energy saving," *IEEE transactions on intelligent transportation systems*, vol. 16, no. 2, pp. 622–631, 2014.
- [12] Z. Pan, M. Chen, S. Lu, Z. Tian, and Y. Liu, "Integrated timetable optimization for minimum total energy consumption of an ac railway system," *IEEE Transactions on Vehicular Technology*, vol. 69, no. 4, pp. 3641–3653, 2020.
- [13] X.-C. Ran, S.-K. Chen, G.-H. Liu, and Y. Bai, "Energy-efficient approach combining train speed profile and timetable optimisations for metro operations," *IET Intelligent Transport Systems*, vol. 14, no. 14, pp. 1967–1977, 2020.
- [14] H. Douglas, C. Roberts, S. Hillmansen, and F. Schmid, "An assessment of available measures to reduce traction energy use in railway networks," *Energy Conversion and Management*, vol. 106, pp. 1149–1165, 2015.
- [15] Z. Tian, N. Zhao, S. Hillmansen, S. Su, and C. Wen, "Traction power substation load analysis with various train operating styles and substation fault modes," *Energies*, vol. 13, no. 11, p. 2788, 2020.
- [16] J. T. Haahr, D. Pisinger, and M. Sabbaghian, "A dynamic programming approach for optimizing train speed profiles with speed restrictions and passage points," *Transportation Research Part B: Methodological*, vol. 99, pp. 167–182, 2017.
- [17] N. Zhao, C. Roberts, and S. Hillmansen, "The application of an enhanced brute force algorithm to minimise energy costs and train delays for differing railway train control systems," *Proceedings of the Institution of Mechanical Engineers, Part F: Journal of Rail and Rapid Transit*, vol. 228, no. 2, pp. 158–168, 2014.
- [18] Y. Bocharnikov, A. M. Tobias, C. Roberts, S. Hillmansen, and C. J. Goodman, "Optimal driving strategy for traction energy saving on dc suburban railways," *IET Electric Power Applications*, vol. 1, no. 5, pp. 675–682, 2007.
- [19] H. W. Dommel and W. F. Tinney, "Optimal power flow solutions," *IEEE Transactions on power apparatus and systems*, no. 10, pp. 1866–1876, 2007.
- [20] N. M. Peterson, W. F. Tinney, and D. W. Bree, "Iterative linear ac power flow solution for fast approximate outage studies," *IEEE Transactions on Power Apparatus and Systems*, no. 5, pp. 2048–2056, 1972.
- [21] B. Mohamed, P. Arbolea, and C. Gonzalez-Moran, "Modified current injection method for power flow analysis in heavy-meshed dc railway networks with nonreversible substations," *IEEE Transactions on Vehicular Technology*, vol. 66, no. 9, pp. 7688–7696, 2017.
- [22] A. S. Zamzam and K. Baker, "Learning optimal solutions for extremely fast ac optimal power flow," in *2020 IEEE international conference on communications, control, and computing technologies for smart grids (SmartGridComm)*. IEEE, 2020, pp. 1–6.
- [23] Y. Zhou, B. Zhang, C. Xu, T. Lan, R. Diao, D. Shi, Z. Wang, and W.-J. Lee, "A data-driven method for fast ac optimal power flow solutions via deep reinforcement learning," *Journal of Modern Power Systems and Clean Energy*, vol. 8, no. 6, pp. 1128–1139, 2020.
- [24] K. Panou, P. Tzieropoulos, and D. Emery, "Railway driver advice systems: Evaluation of methods, tools and systems," *Journal of Rail Transport Planning & Management*, vol. 3, no. 4, pp. 150–162, 2013.
- [25] M. L. Ambrus, S. Hillmansen, and Z. Tian, "Algorithmic energy management in constrained railway traction networks: A systematic review," 2026. [Online]. Available: <https://arxiv.org/abs/2604.06369>
- [26] W. Mingli, C. Roberts, and S. Hillmansen, "Modelling of ac feeding systems of electric railways based on a uniform multi-conductor chain circuit topology," in *IET conference on railway traction systems (RTS 2010)*. IET, 2010, pp. 1–5.
- [27] B. Mellitt, C. Goodman, and R. Arthurton, "Simulator for studying operational and power-supply conditions in rapid-transit railways," in *Proceedings of the Institution of Electrical Engineers*, vol. 125, no. 4, IET, 1978, pp. 298–303.
- [28] H. Hu, Y. Liu, Y. Li, Z. He, S. Gao, X. Zhu, and H. Tao, "Traction power systems for electrified railways: evolution, state of the art, and future trends," *Railway Engineering Science*, vol. 32, no. 1, pp. 1–19, 2024.
- [29] CENELEC, *Railway Applications — Supply Voltages of Traction Systems*, European Committee for Electrotechnical Standardization, Brussels, Belgium, 2004, EN 50163:2004+A1:2007+A2:2020.

- [30] ———, *Railway Applications — Fixed Installations and Rolling Stock — Technical Criteria for the Coordination Between Electric Traction Power Supply Systems and Rolling Stock to Achieve Interoperability — Part 1: General*, European Committee for Electrotechnical Standardization, Brussels, Belgium, 2022, EN 50388-1:2022.
- [31] R. D. White, “AC 25 kV 50 Hz electrification supply design,” in *7th IET Professional Development Course on Railway Electrification Infrastructure and Systems (REIS 2015)*. IET, 2015.
- [32] Y. Oura, Y. Mochinaga, and H. Nagasawa, “Railway electric power feeding systems,” *Japan railway & transport review*, vol. 16, no. 10, pp. 48–58, 1998.
- [33] B. Bhargava, “Railway electrification systems and configurations,” in *1999 IEEE Power Engineering Society Summer Meeting. Conference Proceedings (Cat. No. 99CH36364)*, vol. 1. IEEE, 1999, pp. 445–450.
- [34] RSSB, “Feasibility of smart traction energy management on the western route,” 2024. [Online]. Available: <https://www.rssb.co.uk/research-catalogue/CatalogueItem/T1270>
- [35] T. Ratriyomchai, S. Hillmansen, and P. Tricoli, “Recent developments and applications of energy storage devices in electrified railways,” *IET Electrical Systems in Transportation*, vol. 4, no. 1, pp. 9–20, 2014.
- [36] M. Shang, Y. Zhou, Y. Mei, J. Zhao, and H. Fujita, “Energy-saving train operation synergy based on multi-agent deep reinforcement learning on spark cloud,” *IEEE Transactions on Vehicular Technology*, vol. 72, no. 1, pp. 214–226, 2022.